Influence of infill percentage on the mode I fracture toughness of adhesively bonded Double Cantilever Beam joints with Additively Manufactured PLA adherends

To cite this article: F Moroni *et al* 2021 *IOP Conf. Ser.: Mater. Sci. Eng.* **1038** 012054

Influence of infill percentage on the mode I fracture toughness of adhesively bonded Double Cantilever Beam joints with Additively Manufactured PLA adherends

F Moroni[1], A Pirondi[1], L Bergonzi[2] and M Vettori[2]

[1]Dipartimento di Ingegneria e Architettura, Università di Parma, Parco Area delle Scienze 181/A, 43124 Parma, Italy
[2]MaCh3D srl, V.Le Duca Alessandro 42, 43121 Parma, Italy

E-mail: alessandro.pirondi@unipr.it

Abstract. Adhesive bonding can disclose the possibility to additively manufacture (AM) smaller, highly optimized objects to be bonded in post-production into/onto larger components. However, the infill shape and percentage can influence the fracture toughness of a bonded joint as it emerges from the literature Since the choice of the infill yields also a significant impact on manufacturing time, it is important to assess clearly its influence on bonded joint strength in order to balance strength and manufacturing issues. Therefore, in this work the Mode I fracture toughness of PLA bonded joints obtained by FFF will be assessed as a function of infill percentage, from solid (100% infill) to 20% infill. Test will be done using a Double Cantilever Beam (DCB) joint bonded with a PolyUrethane (PU), room temperature-curing adhesive.

1. Introduction

While several investigations are nowadays aimed at improving Additive Manufacturing (AM) processes, the Design for Additive Manufacturing (DfAM) is pointing out the convenience of realizing small-size, highly optimized parts to be later assembled into/onto larger components, for example for improving productivity and robustness of the process using several, parallel-working 3D printers [1].

Therefore, one of the next challenges is the choice of a suitable assembly technology for AM components. In this context, adhesive bonding offers some valuable advantages such as it does not cause the heating of the parts to be joined, preserving the dimensional accuracy [2] as well as the AM material microstructure and strength. Moreover, heterogeneous material joints can be readily manufactured [3]. In [4], a method was proposed to select structural adhesives for polymeric AM parts. This work was followed by others that focused on tailoring AM adherends in order to obtain an improvement in joint strength. In [5], the Young's modulus of the adherends was graded through the thickness by a multi-material printer, with the objective to lower peel and shear stress concentration that arises at single-lap joint ends. The same objective was pursued in [6], but using Liquid Deposition Modelling to lay down a Young's modulus-graded adhesive layer. Cavities through the thickness of the adherend were realized in [7] to cause crack trapping in Double Cantilever Beam joints. However, this latter work brings in a point that is any infill shape and percentage can influence the fracture toughness of a bonded joint. Since the choice of the infill yields also a significant impact on manufacturing time, it is important to assess clearly its influence on bonded joint strength in order to balance strength and manufacturing issues. Therefore, in this work the Mode I fracture toughness of PLA bonded joints obtained by Fused Filament

Fabrication (FFF) will be assessed as a function of infill percentage, from solid (100% infill) to 20% infill. Test will be done using a Double Cantilever Beam (DCB) joint bonded with a PolyUrethane (PU), room temperature-curing adhesive.

2. Experimental methodology

2.1. Materials and bonding procedure

PLA adherends were manufactured using a fused filament fabrication (FFF) Witbox 1 printer (BQ, Madrid, Spagna). The tensile behavior of PLA has been characterized using a servomechanical MaCh3D testing machine (MaCh3D srl, Parma, Italy) at a constant crosshead speed of 5 mm/min using a MTS 632 31F-24 extensometer (MTS Systems Corporation, Eden Prairie, USA) to record strain. The engineering stress-strain data are reported in Figure 1. The Young's modulus resulted E = 2936 MPa.

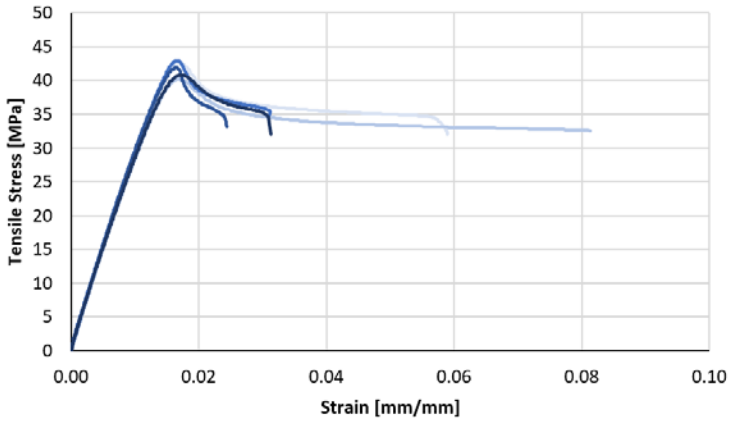

Figure 1. Tensile behavior of PLA.

The DCB geometry is shown in Figure 2 along with the infill shape as generated from CURA 4.6.1 software. Four different values of the infill were considered, that are reported in Table 1 along with the infill setup parameters (p = infill step, t_i = infill wall thickness, t_e = outer wall thickness).

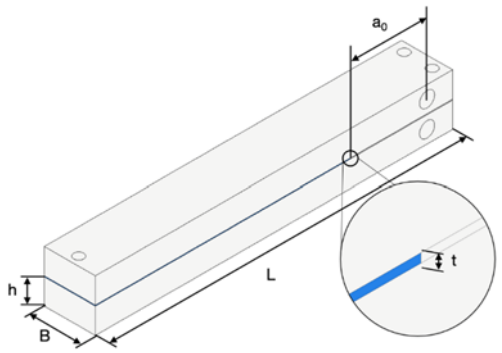

h [mm]	B [mm]	L [mm]	a_0 [mm]	t [mm]
10.0	20.0	140.0	30.0	0.3

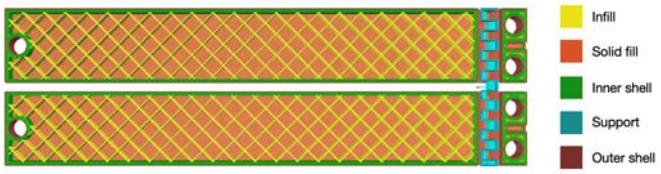

Figure 2. Overall joint geometry and infill shape.

It is worth to underline that when a nominal infill is set in CURA 4.6.1, it corresponds to the effective infill reported in Table 1 that is calculated according to the equation:

$$\text{Effective infill} = 1 - \frac{(p - t_i)^2}{p^2} \quad (1)$$

Table 1. Infill parameters.

Nominal infill (%)	p [mm]	t_i [mm]	t_e[mm]	Effective infill (%)
100	-	-	-	100
60	1.33	0.4	1.2	51
40	2	0.4	1.2	36
20	4	0.4	1.2	19

The adherends were printed with faces to be bonded parallel to the build plane in order to have a morphology such as that studied in [8]. The surface roughness is characterized by the parameter Sa, measured according to ISO 25178-2:2012 with a CCI 3D optical profilometer (Taylor Hobson, Leicester, UK). For the print setup that yielded partially cohesive fracture and the best joint performance in [8], Sa = 15.4 μm .Adherends have been printed one pair at a time to minimize variations due to the different position on the printing table. Support material, to be removed after printing, was necessary to obtain the cylindrical loading hole.

The room temperature-curing PolyUrethane two-components adhesive Teroson PU 9225, supplied by Henkel, was chosen according to the results obtained by [4]. Bulk tensile properties were characterized by testing an ASTM D638 Type IV specimen [9] obtained by pouring adhesive into a PolyTetraFluoroEthylene (PTFE) mould; the main characteristics are reported in Table 2.

Table 2. Teroson PU9225 tensile properties.

Young's Modulus E_A [MPa]	**Poisson's Ratio ν_A**	**Ultimate Strength Rm_A [MPa]**
576.9	0.33	13.3

The bonding procedure encompassed the following steps:

- cleaning with Loctite 7030; the surface was not mechanically/physically/chemically treated in order to preserve the as-built surface morphology;
- placing of a 0.3 mm calibrated foils at adherend ends (Figure 3a);
- placing of a polyester sheet at one end of the adherend to create an initial 30 mm long crack;
- distributing adhesive (Figure 3a);
- closing of the joint by tightening bolts placed in holes at the adherends ends (Figure 3b);
- curing at room temperature for at least one day before testing.

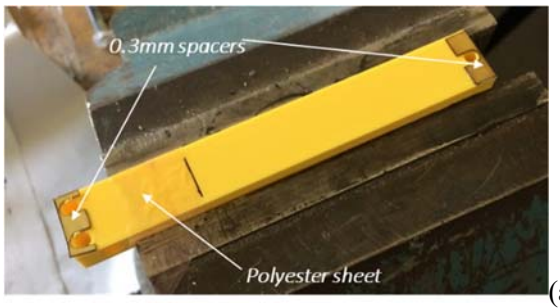

(a)

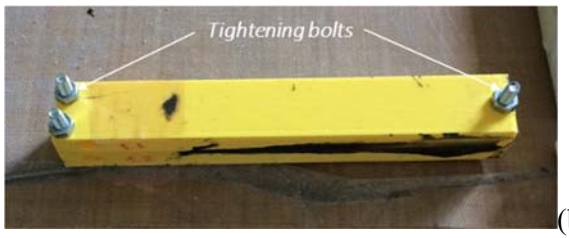

(b)

Figure 3. Bonding procedure: placing of spacers and polyester sheet (a); closing of the joint by tightening bolts (b).

2.2. Testing and data reduction

The fracture tests have been done under displacement control in a MTS servohydraulic machine equipped with a 1 kN load cell. Crack Mouth Opening Displacement (CMOD), δ, has been recorded using a clip-gage. The machine crosshead displacement was set to 6 mm/min and partial unloadings have been performed at given intervals of displacement in order to monitor the specimen compliance, necessary to evaluate the crack length. Three repetitions were done for each infill.

The compliance-crack length relationship was established via Finite Element Analysis (FEA) with a 2D model and an equivalent orthotropic material behavior. The term "equivalent" is used as the adherend exhibit orthotropy with respect to the loading conditions tested as a result of both the FFF fabrication method and the presence of a non-solid infill, while the PLA material is *per se* isotropic. The equivalent orthotropic behavior has been characterized by three-point bending (3PB) test done at different spans. The compliance of an orthotropic beam subject to 3PB, C_{3PB}, is represented by the formula:

$$C_{3PB} = \frac{v}{P} = \frac{(L_s/2)^3}{6E_f I} + 0.6\frac{L_s/2}{GBh} \tag{2}$$

where P is the load, v is the load point displacement, L_s the span length, I the area moment of inertia of the beam section, B and h width and height of the beam, respectively, and E_f and G the equivalent flexural and shear moduli to be determined by least square error minimization with respect to the experimental values of compliance recorded at four different span lengths. The results obtained for the four different infills are shown in Figure 4.

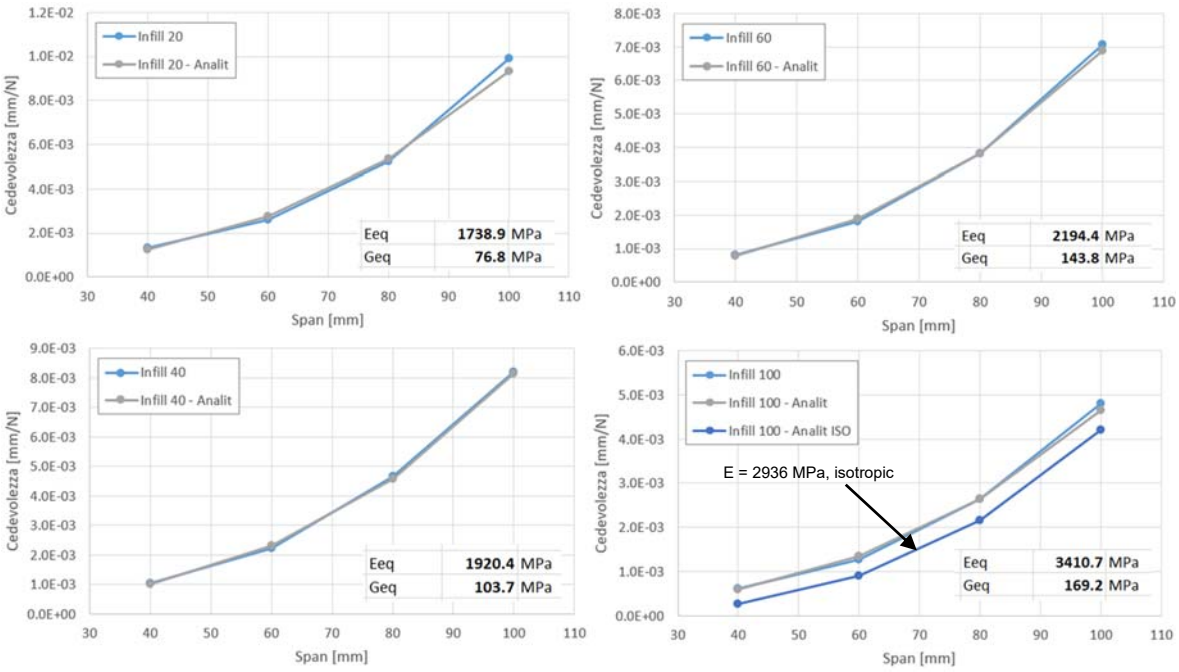

Figure 4. Values of E_f and G for the different infills.

It is worth to underline that the shear modulus G is for all the infills is more than one order of magnitude lower than the flexural one, E_f, making the contribution of shear to the bending stiffness non-negligible even for slender beams like the one use in the present DCB joints. The crack length vs. compliance calibration obtained by 2D FEA using the E_f and G for the different infills is finally shown in Figure 5. The FEA discrete points have been then approximated with a 5th order polynomial function. In order to keep a good correlation coefficient between the polynomial and the discrete data, the range of fitting has been split into two partially overlapping domains, i.e. from 20 to 48 mm and from 38 to 92 mm.

The mode I strain energy release rate G_I has also been evaluated by 2D FEA using the contour integral method and the numerical values have been fit with a 4th degree polynomial expression, with the range of fitting split into two partially overlapping domains as in the case of the compliance. It is worth to

remark that the numerical G_I falls within a few percent difference from the theoretical model of De Moura et al. [10]:

$$G_I = \frac{6P^2}{B^2 h}\left(\frac{2a_e^{\,2}}{E_f h^2} + \frac{1}{5G}\right) \tag{3}$$

where a_e has the meaning of an effective crack length taking into account inelastic and damage phenomena at the crack tip, that in the comparison with 2D FEA has been taken equal to the crack length simulated in the numerical model.

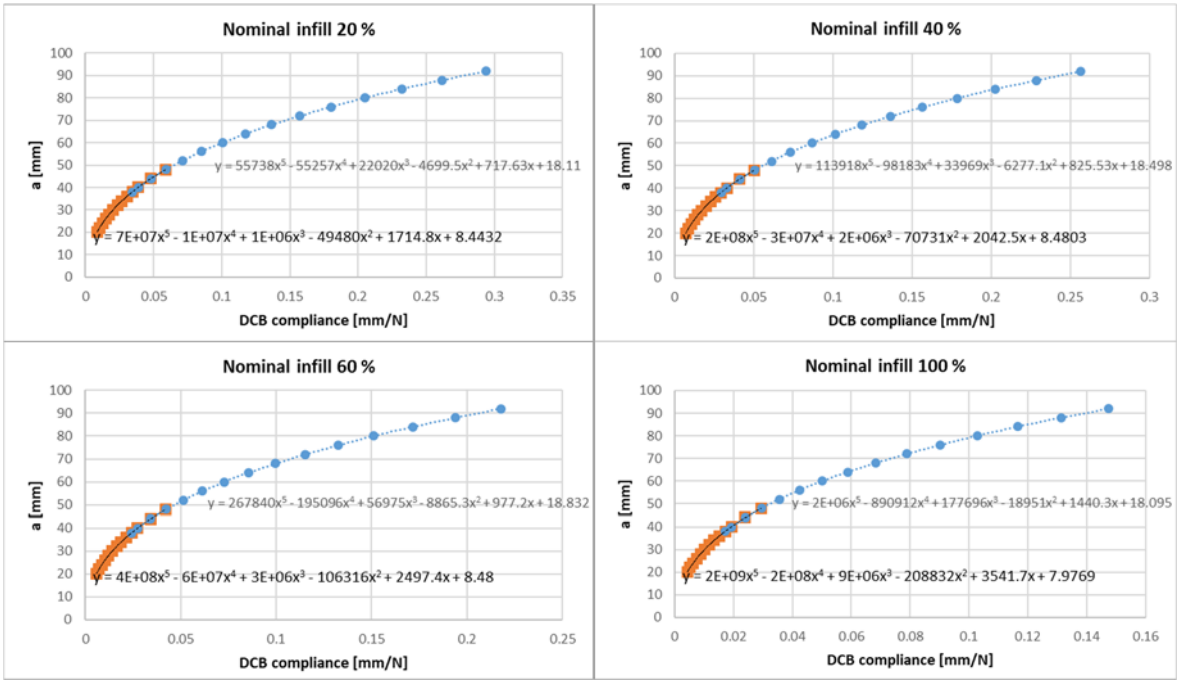

Figure 5. Crack length vs. compliance calibration of the DCB joints.

3. Results and discussion

3.1. Fracture surface

Fracture surfaces of samples with different infills are shown in Figure 6, where the crack propagation region is delimited by the red lines and the direction is from right to left in the figure. In all cases the fracture leaves a layer of adhesive on both surfaces, therefore failure can be said cohesive even though the crack tends to run close to one the interfaces. Most important is that, being the mechanism similar for all the infills, the results in terms of mode I fracture toughness, G_{Ic}, can be compared.

3.2. Force-CMOD and fracture toughness

The values of Force vs. CMOD recorded in the experiments are shown in Figure 7. The trends are not very much different from each other, except that values at 60 % nominal infill are slightly lower and there is one experiment at 100% infill that exhibit clearly a higher force. Since the initial crack length is practically the same for all tests, these differences should be reflected into the G_{Ic} values. From the point of view of data reduction, only the points after the force peak were elaborated since they correspond to a stationary crack propagation and more or less stable values of fracture toughness.

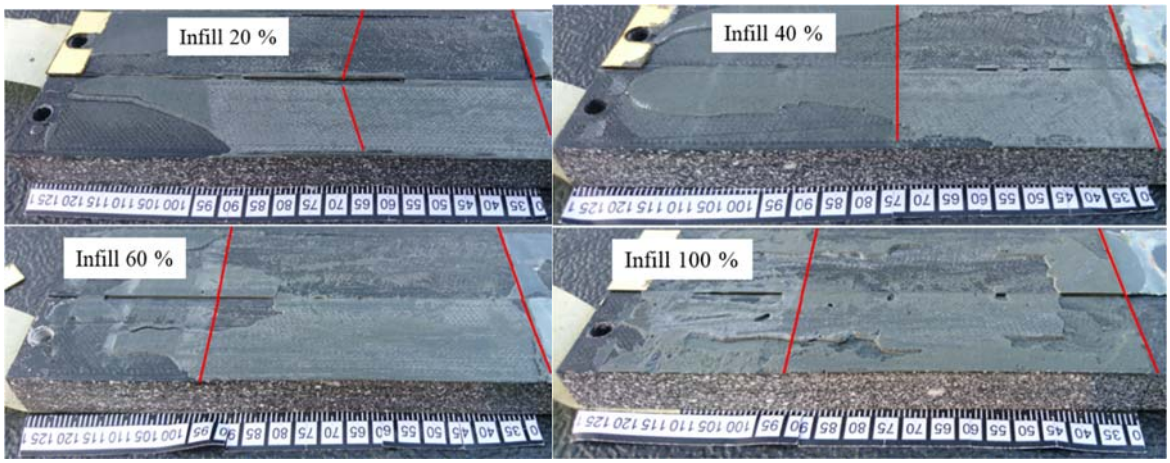

Figure 6. fracture surfaces of joints with different infills.

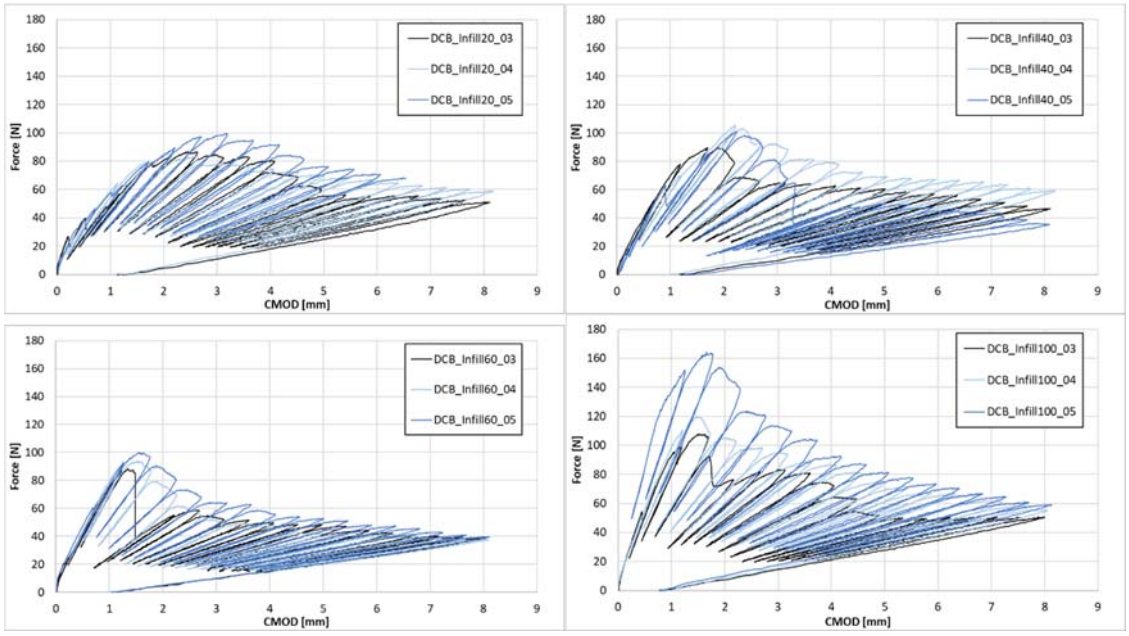

Figure 7. Force vs. CMOD of the DCB tests at different infills.

The fracture toughness values for the three repetitions at different infills are presented in Figure 8. The scatter between the repetitions can be partly related to the failure mechanism, where the crack does not run in the middle of the adhesive layer but close to the adherend-adhesive interface, being therefore the measured fracture toughness value more susceptible to local conditions and to the jumps that the crack can manifest running from close to an interface to close to the opposite one.

The fracture toughness of the different infills has been compared by taking the average and the standard deviation of all the three repetitions for each infill. The G_{Ic} vs. effective infill diagram is given in Figure 9. The average values show a decreasing trend for increasing infill percentage in the range 19 to 51% effective infill (20-60% nominal), while with a bulky specimen the fracture toughness raises up to the value of the lower infills. Accounting for the scatter, represented by the error bars of +/- one standard deviation around the average value, the two lower infills and the bulky specimen are not significantly different from a statistical point of view, while the intermediate 51% infill (60% nominal) seems to be definitely lower than the other. A general statement coming out from the analysis of the

results is that basically there are no contraindications to minimize the infill, hence to minimize the manufacturing time with respect to the values of the fracture toughness exhibited by the joints.

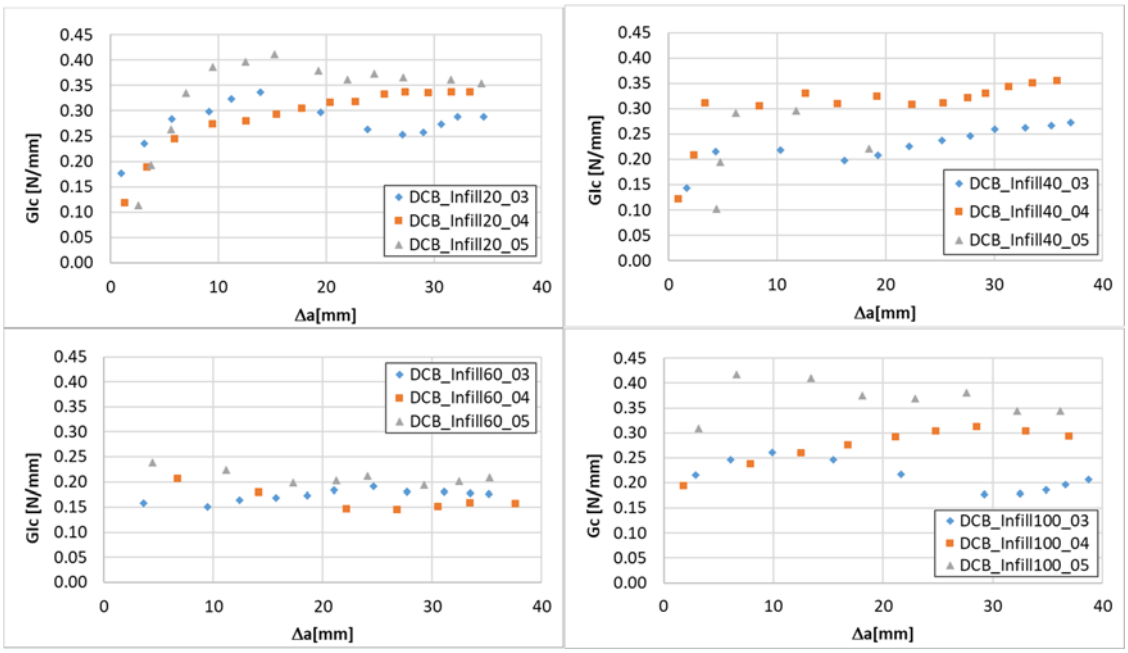

Figure 8. Fracture toughness as a function of crack propagation and at different infills.

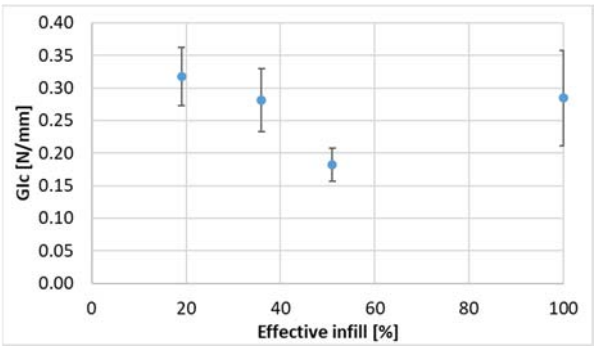

Figure 9. Fracture toughness average and standard deviation at different infills.

4. Conclusions

In this work adherend for DCB (Double Cantilever Beam) joints were produced with four different percentages of internal filling, 20, 40, 60 and 100% respectively, in order to evaluate the effect on the fracture toughness in Mode I of joints bonded with Teroson PU9225. The main conclusions can be summarized in the following points:

- the fracture mode has proved to be cohesive towards the interface in all cases, which are therefore comparable in quantitative terms with respect to fracture toughness;
- the average value of fracture toughness shows a non-monotonous trend as the infill increases;
- joints with adherends having lower infill percentages yield a fracture toughness statistically comparable to that of joints with bulky adherends: there are basically no contraindications to minimizing the infill and therefore maximizing the production rate.

  As a future work, tests are planned at a nominal infill value of 80%, in order to evaluate the trend of fracture toughness also in the 60-100% range.

References

[1] Bürenhaus F, Moritzer E and Hirsch A 2019 Adhesive bonding of FDM-manufactured parts made of ULTEM 9085 considering surface treatment, surface structure, and joint design *Welding in the World* **63**(6) 1819.
[2] Butt J and Bhaskar R 2020 Investigating the Effects of Annealing on the Mechanical Properties of FFF-Printed Thermoplastics *J Manuf Mat Proc* **4**(2) 38.
[3] Kariz M, Kuzman M K, and Sernek M 2017 Adhesive bonding of 3D-printed ABS parts and wood *J Adhes Sci Tech* **31**(15) 1683.
[4] Arenas J M, Alía C, Blaya F, and Sanz A 2012 Multi-criteria selection of structural adhesives to bond ABS parts obtained by rapid prototyping *Int J Adhes Adhes* **33** 67.
[5] Ubaid J Wardle B L and Kumar S 2018 Strength and Performance Enhancement of Multilayers by Spatial Tailoring of Adherend Compliance and Morphology via Multimaterial Jetting Additive Manufacturing Sci Rep **8**(1) 13592.
[6] Sekiguchi Y Nakanouchi M Haraga K Takasaki I and Sato 2019 C Experimental investigation on strength of stepwise tailored single lap adhesive joint using second-generation acrylic adhesive via shear and low-cycle shear tests *Int J Adhes Adhes* **95** 1024.
[7] Morano C Zavattieri P and Alfano M 2020 Tuning energy dissipation in damage tolerant bio-inspired interfaces *J Mech Phys Solids* 1039.
[8] Bergonzi L Frascio M Vettori M Moroni F Pirondi A and Avalle M 2019 Evaluation of surface roughness influence on the strength of structural adhesive joints between additively manufactured adherends *ESIAM19*, 9-11 September 2019, Trondheim, Norway.
[9] *ASTM D638-14 Standard Test Method for Tensile Properties of Plastics* 2014 ASTM International, West Conshohocken, PA, USA.
[10] de Moura M F S F Morais J J L e Dourado N 2008 A new data reduction scheme for mode I wood fracture characterization using the double cantilever beam test *Eng Fract Mech*. **75**(13) 3852.